



Diffusion bonding of Zr-2.5Nb zirconium alloy and 304L stainless steel with Nb/Ni hybrid interlayer

Hong Wang^a, Zhen Wang^a, Gang Chen^a, Lingbao Ren^b, Tianbao Tan^a, Yangyang Guo^c, Yan Liu^a, Houhong Pan^{a,*}

^a Key Laboratory of Advanced Technologies of Materials, Ministry of Education China, School of Materials Science and Engineering, Southwest Jiaotong University, Chengdu, Sichuan 610031, PR China

^b Center for Advancing Materials Performance from the Nanoscale, State Key Laboratory for Mechanical Behavior of Materials, Xi'an Jiaotong University, Xi'an, Shaanxi 710049, PR China

^c Northwest Institute for Non-Ferrous Metal Research, Xi'an, Shaanxi 710016, PR China

ARTICLE INFO

Keywords:

Diffusion
Welding
Microstructure
Zirconium alloy
Stainless steel
Hybrid interlayer

ABSTRACT

Diffusion bonding of Zr-2.5Nb zirconium alloy and 304L stainless steel with Nb and Ni hybrid interlayer was performed at 850–1050 °C under 4 MPa for 30 min. From 304L side to Zr-2.5Nb side, the typical interfacial structure of the 304L/Ni/Nb/Zr-2.5Nb joints was.

(Ni, Cr, Fe) solid solution/Ni/Ni₃Nb IMCs/Nb/(Zr, Nb) solid solution. Of the five layers, the nano-hardness of Ni₃Nb IMCs layer was the highest, reaching ~9.22 GPa for the joint bonded at 1000 °C. With the increase of bonding temperature, the shear strength of the joint increased first and then decreased, and the maximum strength of 84.4 MPa was obtained at 1000 °C. For the joint bonded at 1000 °C, the fracture location was between the residual Ni layer and Ni₃Nb IMCs layer, and the fracture type was a mixture of brittle fracture and ductile fracture.

1. Introduction

Zr-2.5Nb zirconium (Zr) alloy is an indispensable material in the field of nuclear power due to its excellent high-temperature mechanical properties, good corrosion resistance, and is used for pressure tubes in the nuclear reactor [1]. As a rare metal, Zr alloy is expensive and is only used for in-core of reactor, while stainless steel (SS) with low price is used for out-of-core of reactor [2]. Therefore, the effective joining between Zr alloy and SS is of great significance for the safe run of nuclear reactors. When Zr alloy was directly joined to SS by fusion welding or by diffusion bonding, brittle Zr-Fe, Zr-Cr and Zr-Ni intermetallic compounds (IMCs) were easily formed, which weakened the mechanical properties of the joints [3,4]. Diffusion bonding with interlayer is an excellent method to join dissimilar materials which is easy to form brittle IMCs. Various interlayer metals such as Ti [5], Ta [6], Cu [7], Fe [8], Ni [9], Ni/Ti [10], Ag/Ti [11] had been used in diffusion bonding of Zr alloy and SS. Nb and Ni is the main alloying element of Zr-2.5Nb Zr alloy and 304L SS, respectively, and has good metallurgical compatibility with Zr and Fe, respectively. When using Nb and Ni as the interlayers, only Ni-Nb IMCs were formed at the Nb/Ni interface, while no

IMCs were formed at the Ni/304L and Nb/Zr-2.5Nb interfaces with a result of reducing IMCs type of the bonded joint. In the present work, diffusion bonding of Zr-2.5Nb Zr alloy and 304L SS with Nb/Ni hybrid interlayer was carried out, and the research was focused on characterization of the microstructure and the mechanical properties of the bonded joints.

2. Experimental methods

Zr-2.5Nb Zr alloy and 304L SS with the dimensions of 10 × 10 × 5 mm³ were used as the substrates, and 30 μm thickness of Nb foil and 45 μm thickness of Ni foil were used as the diffusion interlayers. All the faying surfaces were grinded and polished, and finally ultrasonic cleaned. The diffusion couple was assembled as the order of 304L/Ni/Nb/Zr-2.5Nb. The bonding conditions were the bonding temperature of 850–1050 °C under the bonding pressure of 4 MPa for the bonding time of 30 min. During bonding, the assembly specimen was heated to the bonding temperature at a heating rate of 20 °C/min. After bonding, the bonded sample was furnace cooled to room temperature. In addition, the material compositions and the characterization methods were

* Corresponding author.

E-mail address: houhongpan@home.swjtu.edu.cn (H. Pan).

<https://doi.org/10.1016/j.matlet.2022.132652>

Received 5 April 2022; Received in revised form 7 June 2022; Accepted 13 June 2022

Available online 14 June 2022

0167-577X/© 2022 Elsevier B.V. All rights reserved.

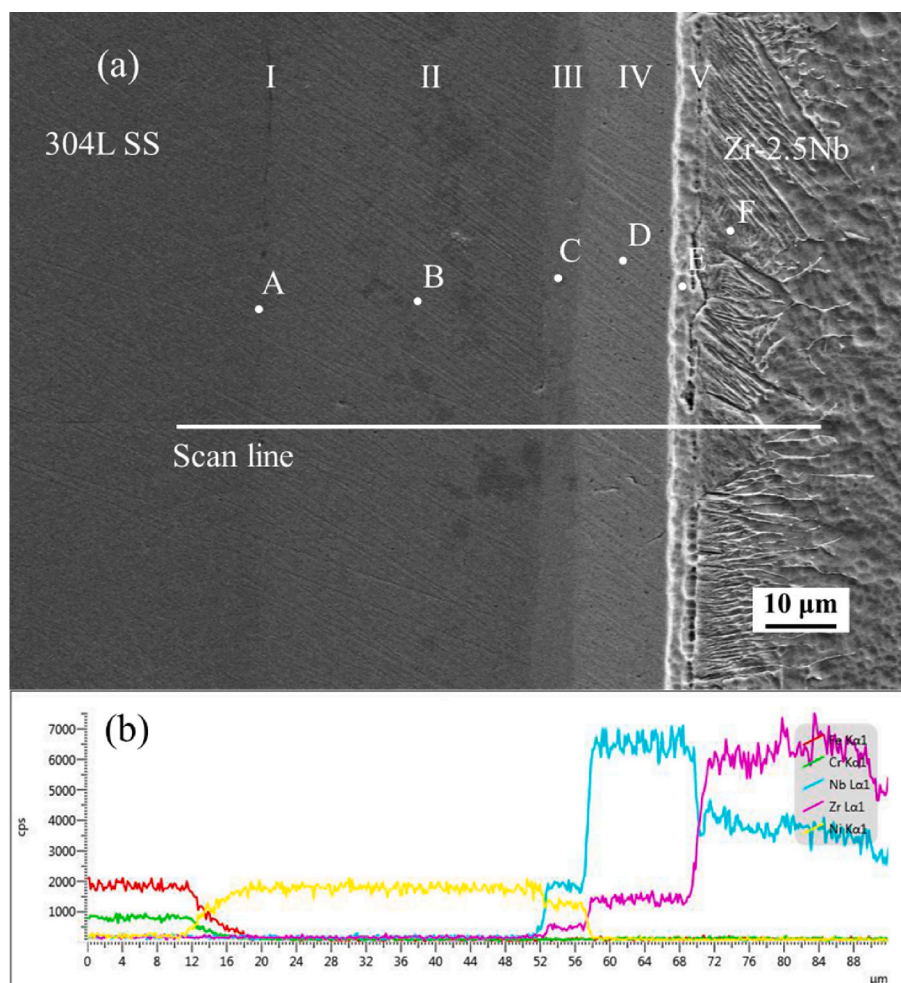


Fig. 1. (a) SEM image and (b) EDS line scanning of the joint bonded at 1000 °C.

Table 1
EDS analysis of points A-F in Fig. 1(a).

Points	Elements (at. %)					Possible phases
	Fe	Ni	Nb	Zr	Cr	
A	41.64	50.92	–	–	7.44	(Fe, Ni, Cr) solid-solution
B	0.20	99.80	–	–	–	α-Ni
C	–	74.40	25.40	0.20	–	Ni ₃ Nb
D	–	–	99.58	0.42	–	α-Nb
E	1.10	–	17.40	81.50	–	Zr (Nb) solid-solution
F	–	–	8.40	91.60	–	Zr (Nb) solid-solution

detailed in the [Supplementary Information](#).

3. Results and discussion

The joints bonded at the different bonding temperature had identical microscopic morphology and layered structure. Therefore, the joint bonded at 1000 °C was selected as an example to investigate the microstructure of the joint. Fig. 1 shows the microstructure and the EDS line scanning results of the joint bonded at 1000 °C. As Fig. 1 showed, the diffusion reaction region of the joint was divided into five layers, marked as I, II, III, IV and V. The EDS point analysis of each layer in Fig. 1(a) was listed in Table 1. The contents of Cr and Fe elements in the layer I were gradually decreased, while that of the Ni element was gradually increased, indicating this layer as a transition region of 304L SS and Ni interlayer. Next to layer I, layer II had continuous composition of Ni (99.8 at.%), Fe (0.2 at.%), which indicated that it was the

unreacted Ni. The layer III was observed to contain Ni (74.4 at.%), Nb (25.4 at.%) and Zr (0.2 at.%) and the stoichiometric proportion of Ni to Nb was approximately 3:1. Combined with the Ni-Nb binary phase diagram [12], the layer III could be judged as a Ni₃Nb IMCs layer. Close to the layer III, layer IV had a constant composition of Nb and Zr. According to the EDS results of point D (Nb 99.58 at.% and Zr 0.42 at.%), the layer IV was identified as residual Nb. Adjacent to layer IV, the layer V had a continuous concentration gradient distribution of Nb and Zr, which could be judged as a Nb-Zr solid solution layer.

The nano-hardness of the joint bonded at 1000 °C is shown in Fig. 2 (a). The average nano-hardness of 304L SS, Ni interlayer (layer II), Nb interlayer (layer IV) and Zr alloy were ~3.37 GPa, ~2.62 GPa, ~1.80 GPa and ~3.13 GPa, respectively. It can be seen from Fig. 2(a) that the hardness of layer I (~2.81 GPa) showed a slightly increase compared to layer II, which could be attributed to the solution strengthening caused by the interdiffusion of Cr, Ni, and Fe atoms in this region. Similarly, the hardness of layer V (~3.51 GPa) was higher than that of layer IV with the interdiffusion of Nb and Zr atoms in this region. Due to the formation of Ni₃Nb IMCs, the hardness of layer III was the highest with a hardness of ~9.22 GPa, which was higher than that of layer II and layer IV. The shear strength of the joints bonded at the different bonding temperatures is shown in Fig. 2(b). It can be known from Fig. 2(b) that the shear strength increased with the bonding temperature increasing until 1000 °C, and then decreased above 1000 °C. The shear strength of the joint bonded at 850 °C was the lowest with a value of 20.2 MPa, which could be attributed to the insufficient diffusion reaction at the low temperature, while the highest shear strength value of 84.4 MPa was obtained for the joint bonded at 1000 °C.

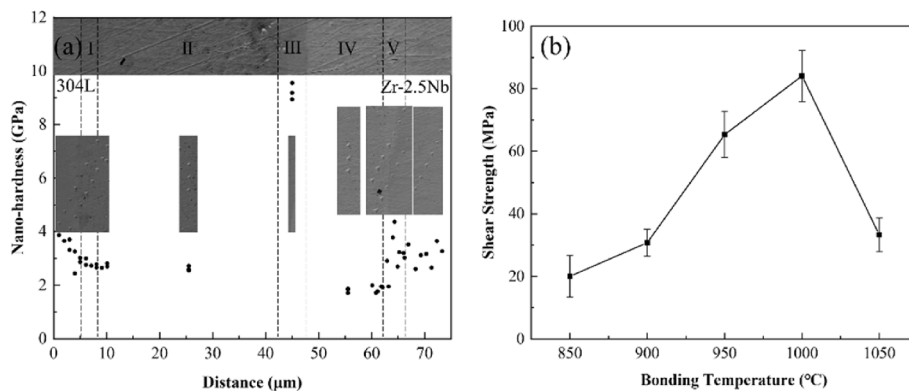


Fig. 2. (a) Nano-hardness of the joint bonded at 1000 °C and (b) shear strength of the joints bonded at different bonding temperatures.

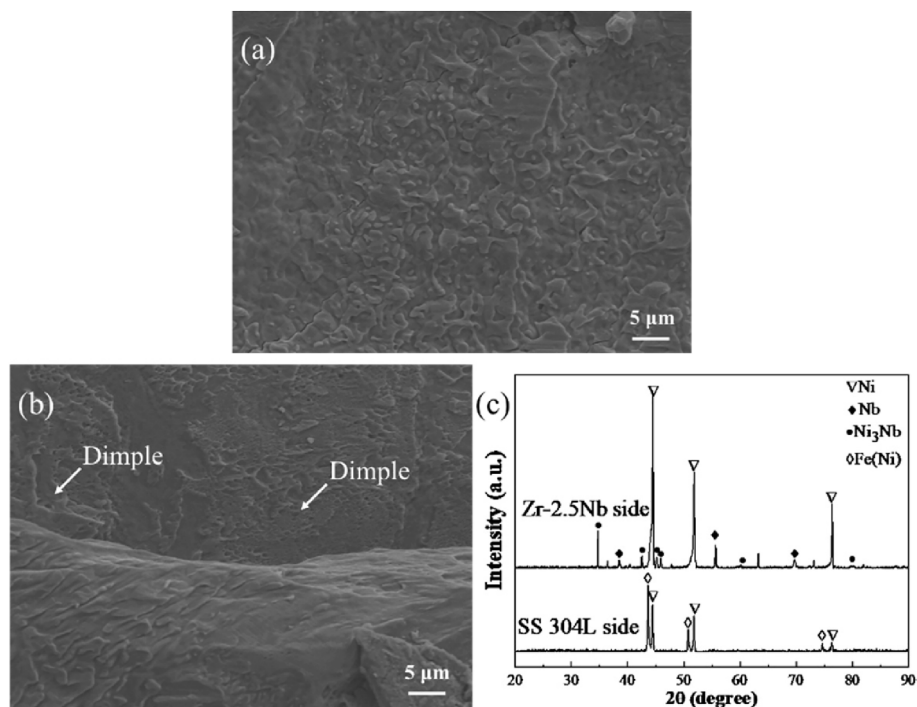


Fig. 3. (a) SEM image at Zr-2.5Nb side, (b) SEM image at 304L side and (c) XRD results on the fractured surface of the joint bonded at 1000 °C.

The SEM micrographs and the XRD results of the fractured surfaces of the joint bonded at 1000 °C are presented in Fig. 3. The shear fractured surface of the Zr-2.5Nb side (Fig. 3(a)) was found to have the characteristics of tearing fracture and transgranular fracture at the same time. It can be also seen from the fractography of the 304L side (Fig. 3(b)) that there were a small number of cleavage steps and scattered shear toughening nests of different sizes on the fractured surface. Therefore, the fracture type of the joint was the mixed fracture of brittle fracture and ductile fracture. XRD results showed (Fig. 3(c)) that Ni, Nb, Ni₃Nb were detected on the fractured surface of Zr-2.5Nb side while Ni and Fe (Ni) were detected on the fractured surface of 304L side. Therefore, it can be concluded that the shear fracture of the joint obtained at 1000 °C was located between the residual Ni layer and Ni₃Nb IMCs layer.

4. Conclusions

In this paper, Zr-2.5Nb Zr alloy and 304L SS were joined by vacuum diffusion bonding with Nb/Ni as the hybrid interlayer. The research results showed that the typical interfacial structure of the 304L/Ni/Nb/Zr-2.5Nb joints was (Ni, Cr, Fe) solid solution/Ni/Ni₃Nb IMCs/Nb/.

(Zr, Nb) solid solution from 304L SS side to Zr-2.5Nb Zr alloy side. In the joint bonded at 1000 °C, the nano-hardness of Ni₃Nb IMCs layer was the highest, reaching ~9.22 GPa. With the increase of the bonding temperature, the shear strength of the joint increased gradually, reaching the maximum strength of 84.4 MPa at 1000 °C, and then decreased above 1000 °C. The shear fractured surface of the joint bonded at 1000 °C was located between the residual Ni layer and Ni₃Nb IMCs layer. The fracture type was a mixture of brittle fracture and ductile fracture.

CRediT authorship contribution statement

Hong Wang: Conceptualization, Formal analysis, Writing – original draft. **Zhen Wang:** Investigation, Methodology. **Gang Chen:** Writing – review & editing. **Lingbao Ren:** Writing – review & editing. **Tianbao Tan:** Writing – review & editing. **Yangyang Guo:** Writing – review & editing. **Yan Liu:** Project administration. **Houhong Pan:** Investigation, Resources, Supervision.

Declaration of Competing Interest

The authors declare that they have no known competing financial interests or personal relationships that could have appeared to influence the work reported in this paper.

Acknowledgments

This work was supported by National Nature Science Foundation of China (No. 52175366), and the 2020 open projects of Key Laboratory of Advanced Technologies of Materials, Ministry of Education China, Southwest Jiaotong University (No. KLATM202003), and China Post-doctoral Science Foundation (No: 2021M692512). And the authors thanks Danli Zhang in Center for Advancing Materials Performance from the Nanoscale for the nanoindentation tests.

Appendix A. Supplementary data

Supplementary data to this article can be found online at <https://doi.org/10.1016/j.matlet.2022.132652>.

[org/10.1016/j.matlet.2022.132652](https://doi.org/10.1016/j.matlet.2022.132652).

References

- [1] J.L. Liu, G.Z. He, A. Callow, K.X. Li, K.L. Moore, H. Nordin, M. Moody, S. Lozano-Perez, C.R.M. Grovenor, *Acta Mater.* 215 (2021), 117042.
- [2] R.L. Klueh, A.T. Nelson, *J. Nucl. Mater.* 371 (2007) 37–52.
- [3] M. Ahmad, J.I. Akhter, M. Akhtar, M. Iqbal, *J. Mater. Sci.* 42 (2007) 328–331.
- [4] H.I. Shaaban, F.H. Hammad, J.L. Baron, *J. Nucl. Mater.* 71 (1978) 277–285.
- [5] J.I. Akhter, M. Ahmad, M. Iqbal, M. Akhtar, M.A. Shaikh, *J. Alloys Compd.* 399 (2005) 96–100.
- [6] M. Ahmad, J.I. Akhter, Q. Zaman, M.A. Shaikh, M. Akhtar, M. Iqbal, E. Ahmed, *J. Nucl. Mater.* 317 (2003) 212–216.
- [7] D. Aboudi, S. Lebaili, M. Taouinet, J. Zollinger, *Mater. Des.* 116 (2017) 386–394.
- [8] H.I. Shaaban, F.H. Hammad, J.L. Baron, *J. Nucl. Mater.* 78 (1978) 431–433.
- [9] H.S. Chen, C.S. Long, T.G. Wei, W. Gao, H.X. Xiao, L. Chen, *Mater. Des.* 60 (2014) 358–362.
- [10] V. Srikanth, A. Laik, G.K. Dey, *Mater. Des.* 126 (2017) 141–154.
- [11] H.H. Pan, B.S. Liu, Y.Y. Guo, Y. Liu, G.F. Quan, *Mater. Lett.* 240 (2019) 185–188.
- [12] T. B. Massalski, J. L. Murray, L. H. Bennett, H. Baker, *Binary Alloy Phase Diagrams*, Vol. 1 and 2, American Society for Metals, Ohio, 1986.